Published in final edited form as:
Clin Neurosurg. 2012 ; 59: 107–113. doi:10.1227/NEU.0b013e31826989ef.

Canine Model of Convection-Enhanced Delivery of Cetuximab Conjugated Iron-Oxide Nanoparticles Monitored with Magnetic Resonance Imaging

Simon Platt, B.V.M.&S., M.R.C.V.S.[1], **Edjah Nduom, M.D.**[2], **Marc Kent, D.V.M.**[1], **Courtenay Freeman, D.V.M.**[1], **Revaz Machaidze, B.S.**[2,4], **Milota Kaluzova, Ph.D.**[2,4], **Liya Wang, M.D.**[3], **Hui Mao, Ph.D.**[3,4], and **Costas G. Hadjipanayis, M.D., Ph.D.**[2,4]

[1]Department of Small Animal Medicine and Surgery, College of Veterinary Medicine, University of Georgia, Athens, GA 30602

[2]Brain Tumor Nanotechnology Laboratory [2], Department of Neurosurgery, Emory University School of Medicine, Atlanta, GA 30322

[3]Department of Radiology and Imaging Sciences, Emory University School of Medicine, Atlanta, GA 30322

[4]Winship Cancer Institute of Emory University, Atlanta, GA 30322

Abstract

Introduction—Visualizing distribution of infused therapeutic agents into the brain by convection-enhanced delivery (CED) is necessary to ensure accurate delivery into target sites. Recently, bioconjugated magnetic iron-oxide nanoparticles (IONPs) have been shown to produce a magnetic resonance imaging (MRI) contrast in the rodent brain after CED permitting direct visualization of nanoparticle distribution and dispersion over time. We have now studied the CED of IONPs in the larger, more clinically relevant, canine brain for assessment of distribution, dispersion, toxicity, and clearance.

Methods—Eight healthy laboratory dogs were infused with either free IONPs (n=4) or cetuximab-conjugated IONPs (cetuximab-IONPs; n=4) at different infusion rates (0.5, 1.0, 3.0, and 5.0 microliters/min) and volumes (180, 300, 360, and 720 microliters). IONP CED was monitored by sequential MRIs (pre-operative, within 12 h, 5 d, 7 d, and 30 d post-operative) and volumes of distribution and dispersion were calculated from the MR images. Toxicity assessment was based on MRI, clinical examination, hematologic/cerebrospinal fluid (CSF) analysis, and brain histopathological evaluation.

Results—Robust delivery and monitoring of IONP distribution in the grey and white matter of the canine brain was achieved by CED and MRI. Quantitative measurements of IONP distribution volumes was achieved by MRI. Distribution volumes were linearly proportional to infusion volumes and dispersion of IONPs occurred 5 d after CED. Use of the slower infusion rates allowed for more uniform initial distribution of IONPs and low infusate leakback of IONPs along the catheter track. No signs of toxicity were found in any animals that underwent IONP or cetuximab-conjugated IONP CED based on physical examination and hematologic/CSF analysis. MRI and histopathologic analysis of brains 30 d after CED revealed near complete clearance of IONPs. Uptake of IONPs by astrocytes and microglia was found adjacent to the catheter sites.

Corresponding Author: Costas G Hadjipanayis, M.D., Ph.D., Dept. of Neurosurgery, Emory University School of Medicine, 1365B Clifton Rd. NE, Suite 6200, Atlanta, GA 30322, USA, chadjip@emory.edu, Phone: +1 (404) 778-3091, Fax: +1 (404) 778-4472.

Conclusions—CED of either free or cetuximab-conjugated IONPs in the canine brain is safe and represents an effective delivery method in a larger animal model. MRI monitoring of distribution and dispersion of IONPs is possible and quantitative after CED. Future studies involving CED of bioconjugated IONPs in canines with spontaneous gliomas may provide a unique and more clinical relevant animal model for targeting infiltrative cancer cells responsible for tumor recurrence.

Keywords

Glioblastoma; Magnetic Nanoparticles; Convection-Enhanced Delivery; MRI; EGFR; Cetuximab; Canine

Introduction

Convection-enhanced delivery (CED) of therapeutic agents has been used in multiple human clinical trials to determine therapeutic efficacy against malignant brain tumors [1,2]. CED has been designed to infuse agents intratumorally and into the surrounding brain parenchyma, bypassing the blood brain barrier (BBB) and avoiding non-specific uptake [3]. The positive pressure gradient established during CED permits fluid convection and enhances the distribution of molecules into brain [4]. Therapeutic agents can be delivered into the brain by CED in high concentrations without toxicity to normal tissue and organs commonly associated with systemic delivery [5]. The use of CED can also allow for therapeutic targeting of infiltrating cancer cells in the normal brain, a major cause for brain tumor recurrence after surgery.

The lack of non-invasive monitoring of CED in the brain for agent distribution and tumor targeting is the single largest impediment to this delivery strategy. Ineffective drug distribution is one major criticism of CED that may compromise malignant brain tumor targeting and therapy [6]. Agent surface properties (cationic charge), large hydrodynamic size, catheter positioning, and high interstitial tumor pressures can compromise agent distribution [4,6–10]. Visualizing distribution of infused agents is necessary to ensure accurate delivery into target sites and provides feedback on catheter placement and control of agent delivery [11,12]. Previous studies have radio-labeled their therapeutic agent, co-infused their agent with radio-labeled albumin (^{123}I-labeled albumin), or used liposomes containing an MRI contrast agent (e.g., gadoteridol) for real-time CED imaging [13–16]. Radio-labeling of therapeutic agents relies on low resolution single-photon emission computerized tomography (SPECT) for agent imaging and also raises concerns of using radioactive materials with CED. Co-infusion of imaging agents with different size and surface properties may not accurately depict actual therapeutic agent distribution and cannot be performed over time.

Recently, CED of magnetic iron-oxide nanoparticles (IONPs; core size of 10 nm) conjugated to an epidermal growth factor receptor deletion mutant (EGFRvIII) antibody have been reported for the therapeutic targeting of human glioblastoma (GBM) in a rodent model [17]. Due to their unique magnetic properties, IONPs serve as a strong MRI contrast agent, enabling monitoring of CED of IONPs directly by MRI for distribution studies in the brain [18]. Distribution of the EGFRvIII antibody-conjugated IONPs within the GBM xenografts was initially observed and the dispersion of the nanoparticles intratumorally and peritumorally in the brain occurred for days after CED. This study demonstrated the feasibility of CED for MRI-assisted effective delivery of IONPs within brain tumors as well the infiltrating cancer cells beyond the tumor mass responsible for tumor recurrence.

Translation of this promising imaging-guided therapeutic approach into human clinical trials requires demonstration of the safety and efficacy of EGFR antibody-conjugated IONP treatment in a larger animal model. Use of a canine model permits feasibility and toxicity evaluation on a scale relevant to human patients. Furthermore, canines with spontaneous gliomas may serve as the most relevant model for testing the efficacy and treatment responses of therapeutic agents since canine tumors present similar features as human glioblastomas. Similar tumor infiltration into the normal brain, clinical MRI features, and tumor cell EGFR over-expression and signaling alterations have been reported in spontaneous canine gliomas [19–22].

In this work, we report our investigation of MRI-assisted CED of IONPs conjugated to cetuximab, a monoclonal antibody specific to the wild-type (wt) EGFR that cross reacts with the EGFRvIII deletion mutant, in a canine model. Volume of distribution (V_D), dispersion (V_{DI}), clearance, and toxicity studies were performed in healthy canines. We demonstrated the feasibility and safety for CED of IONPs to clinically significant areas of the canine brain. Furthermore, the procedure can be monitored directly with MR imaging.

Methods

Experimental Animals

Eight healthy beagle dogs (4 males and 4 females) were used for the experimental protocol. All canine studies were performed at the University of Georgia College of Veterinary Medicine, (CVM-UGA), an AVMA Accredited and Approved College of Veterinary Medicine. The experimental protocol was reviewed and approved by the Institutional Animal Care and Use Committee at the CVM-UGA. All canines were individually housed in concrete runs and maintained on a 12-hour light/dark cycle with a room temperature of 20–22°C. A standard commercial maintenance dry food diet was provided on a daily basis with water provided ad libitum. All animals underwent complete physical and neurological examinations prior to the procedure and daily thereafter until completion of the study. Animal weights were also documented.

Bioconjugated Cetuximab-IONPs

Clinical grade cetuximab (Imclone, Inc.) was obtained from the Winship Cancer Institute of Emory University for conjugation to the IONPs (Figure 1). Amphiphilic triblock copolymer coated IONPs (core size of 10 nm) were obtained from Ocean Nanotech, Inc. (Figure 1). A 1:1 antibody to IONP conjugation was performed. Briefly, activation of the carboxyl groups on the IONPs was performed for conjugation of the cetuximab antibody after addition of an Activation Buffer, ethyl dimethylaminopropyl carbodiimide (EDC) and sulfo-NHS. The EDC/NHS solution was mixed vigorously with the IONPs at 25 C for 15 min. Excess EDC and sulfo-NHS were removed from the activated nanoparticles by three rounds of centrifugation (1,000g) and resuspension in PBS using Nanosep 10K MWCO OMEGA membrane (Pall Life Sciences). The IONPs with activated carboxyl groups were then reacted with cetuximab (50 μl at 2 mg/ml) at 25°C for 2 h, and the reaction mixture was stored at 4°C overnight. Excess antibody was removed by three rounds of centrifugation and resuspension in PBS using 100K MWCO OMEGA membranes. Conjugation efficiency was confirmed by mobility shift in 1% agarose gel and was visualized by staining with 0.25% Coomassie Brilliant Blue in 45% methanol, 10% acetic acid for 1 h, and destaining in 30% methanol, 10% acetic acid overnight (Figure 1). Cetuximab-IONPs or IONPs were suspended in PBS and a concentration of 0.2 mg/ml was used for all canine CED studies.

Canine IONP CED Studies

Two groups of healthy dogs underwent CED of free IONPs (Group 1; N=4) or bioconjugated cetuximab-IONPs (Group 2; N=4) after placement of a single closed-tip catheter (Hermetic Catheter from Integra NeuroSciences) through a 3–5 mm right frontal burr hole approximately 1.5–2 cm into the frontal lobe after general anesthesia (Figure 2). Each catheter was tunneled under the skin and connected to an external programmable reservoir infusion pump (Medtronic Synchromed II, Medtronic Inc.) that was strapped to each animal's head (Figure 2). Each pump was filled with either free IONPs or cetuximab-IONPs. Infusions were performed after programming of the external reservoir pump (Medtronic Synchromed II) utilizing a handheld device. Animals did not require anesthesia for their CED procedures. CED parameters of infusion rate (I_R) and volume (V_i) were programmed. Animals underwent IONP CED at a rate of 0.5, 1.0, 3.0, or 5.0 μl/min for 1, 6, 12, or 24 h. V_i ranged from 180–720 μl.

IONP MRI Distribution Studies

Brain MRI scans were performed on all dogs prior and within 12 h after their CED procedure. Group 1 dogs underwent a brain MRI scan 7 d after CED for initial feasibility studies. Group 2 animals underwent MRI scans at 5 and 30 d after CED to determine IONP volume distribution (V_D), dispersion (V_{DI}), and clearance with lower infusion rates. All MRI experiments were done using a whole body 3T MRI scanner (GE Signa). Under general anesthesia, dogs were placed in sternal recumbency. The head was immobilized in the headcoil and positioned in the isocenter of the magnet. Whole brain scans were performed with T1-weighted spin echo sequence, T2-weighted fast spin echo sequence, T2 weighted flow attenuated inversion recovery (FLAIR) sequence and 3D gradient echo sequence, before and after IONP CED. Since the size of the canine brain approaches that of the human brain, MRI parameters selected for each canine were slightly modified from those of the brain MRI protocol used in human patients at Emory University. The field of view (FOV) of 20 cm, matrix of 256 by 256, slice thickness of 4 mm (no gap) were used in the scan sequences. The scans were performed in the coronal sections.

Region of interest (ROI) analysis was used to determine the V_D of IONPs at different time points after CED. Since IONPs induce hypointensity (signal drop) with T2-weighted imaging (T2WI), the boundaries of each ROI can be drawn manually on each T2WI slice based on the 10% signal loss in each voxel where IONPs were infused. The number of voxels selected based on this criteria were summed from each slice showing IONP induced contrast change. A V_D calculation will be the sum of voxels showing signal drops, as $V_D = N_s*S*R$, where N_s is number of voxel in each slice that have defined signal drops, S is number of slices where voxels are selected, R is in plane resolution in mm. The V_{DI} of the IONPs was determined by the difference in V_D measurements within 12 h after CED and each time point after.

Hematologic and Cerebrospinal Fluid Analysis

Complete blood counts and serum biochemical analyses were performed on all canines 7 d and 30 d after CED. Blood samples were collected by jugular puncture. Cerebrospinal fluid (CSF) analysis was performed 7 d after CED. CSF was obtained by cerebellomedullary cisternal puncture with the animals under general anesthesia.

Brain Histological Analysis

Brains were harvested from all the animals 30 d after their CED procedure and immersed in 10% buffered formalin for 10 d prior to sectioning and histopathologic analysis. Representative sections of the brain were made at each site of CED catheter placement. Five

μm-thick sections were processed for routine hematoxylin/eosin staining as well as Perl's blue staining for iron.

Results

Initial CED and Distribution of IONPs in the Canine Brain

Distribution of the IONPs in the canine brain was achieved for the first time by CED. The direct imaging of delivery of IONPs and intracranial distribution of nanoparticles by T2WI was possible. Both T_1- and T2-weighted imaging confirmed no presence of hemorrhage after each CED procedure.

Group 1 (N=4) received free IONPs (0.2 mg/ml) for 60 minutes at either 3 or 5 μl/min (V_i = 180 μl and I_R = 3.0 μl/min rate in Dogs 1 and 2; V_i = 300 μl and I_R = 5.0 μl/min rate in Dogs 3 and 4) (Figure 3). One dog in Group 1 (Dog #2) was found to have intraventricular distribution of IONPs due to catheter entry into the ventricle (Figure 3) that were not visualized by MRI 7 d later. One dog in Group 2 (Dog #8) was found to have subarachnoid distribution of IONPs since there was no catheter penetration into the brain. Infusate leakback along the catheter was found at the infusion rates of 1, 3, and 5.0 μl/min (Figure 3).

Group 2 (Dogs 5–8) underwent CED of bioconjugated cetuximab-IONPs (0.2 mg/ml) at 0.5 or 1.0 μl/min for 6, 12, or 24 h (V_i = 360 μl and I_R = 0.5 μl/min rate (12 h) in Dog 5; V_i = 720 μl and I_R = 0.5 μl/min rate (24 h) in Dog 6; V_i = 360 μl and I_R = 1.0 μl/min rate (6 h) in Dog 7; V_i = 720 μl and I_R = 1.0 μl/min rate (12 h) in Dog 8) (Figure. 4).

Use of a slower I_R at 0.5 μl/min provided for more uniform distribution of IONPs and low infusate leakback as indicated by the T2WI in Figure 4. Semi-quantitative measurement of areas where IONP induced MRI contrast changes allowed for determining that V_D is linearly proportional to the V_I (Figure 5). The V_D was greatest at 0.5 μl/min for 24 h (289 mm^3).

Dispersion of the cetuximab-IONPs was found 5 days after CED in Group 2 (Figure 5). Greater dispersion was found with use of the slower I_R (0.5 μl/min; V_{DI} 35 mm^3) in comparison to the I_R of 1.0 μl/min (V_{DI} 7 mm^3) (Figure 5).

Toxicity and Clearance of IONPs from the Canine Brain after CED

All dogs showed no signs of toxicity after IONP CED. No neurologic deficits were noted in any of the dogs during the 30 d observation period after their CED procedure and all dogs maintained their normal weight. All dogs showed no abnormalities on cerebrospinal fluid (CSF), hematology, and serum biochemistry analysis 7 d after CED. Hematology and serum biochemistry remained normal at 30 d after CED.

For IONP clearance studies, dogs in Group 2 underwent an additional MRI scan at 30 d. IONP-associated contrast was found on T2WI at 30 d, however at a much smaller volume confirming bioconjugated IONP clearance from the brain (Figs. 4 and 5).

Histopathologic analysis was performed on brain slices harvested from all the animals 30 d after their CED procedure. In all dogs, histopathologic changes were localized to the catheter tracts. Gemistocytic astrocytosis and gitter cells (phagocytizing microglia) were found surrounding the CED catheter sites (Figure 6). Neovascularization and perivascular lymphoplasmacytic infiltration were also found around the catheter tracts. The presence of Fe-containing particles in the brain tissue were confirmed by Perl's blue iron staining (Figure 6). Furthermore, both the astrocytes and microglia contained small spherical iron-

positive particles (Figure 6), indicating the uptake and clearance of the IONPs from the brain by astrocytes and microglia.

Discussion

CED of therapeutic agents into the brain remains a promising treatment strategy for treating glioblastoma (GBM). The ability to directly infuse high concentrations of agents both intratumorally, and peritumorally where infiltrating cancer cells reside, is a main treatment advantage with CED. Current systemic treatment strategies of glioblastoma (GBM) are unable to target tumors in high enough concentration to prevent recurrence with acceptable systemic toxicity. Furthermore, the ability to target infiltrating cancer cells of GBM outside of the main tumor mass where the BBB is intact is unsuccessful with any systemic therapy.

The inability to accurately define the extent and location of CED infusions has led to criticism of this treatment approach for GBM and has compromised the efficacy data of human clinical trials that have been performed [1]. Leakage of infusate into the ventricular or subarachnoid spaces can result in suboptimal tumor targeting and treatment failure [6].

The use of real-time MRI has recently been described during intratumoral CED of liposomal nanoparticles containing the topoisomerase inhibitor CPT-11 and the surrogate marker gadoteridol into spontaneous gliomas in the canine [14] and in the healthy canine brain [23]. Volume of distribution of the infusate, cannula location, and leakage of infusate was determined by real-time MRI. With the real-time MRI approach, canine patients were placed in a stereotactic head frame while under general anesthesia and undergo CED for up to 4 h while in the MRI scanner. The co-infusion of gadoteridol permits immediate infusion distribution assessment and correlation to the treatment agent CPT-11. The MRI contrast effect of the gadoteridol is lost, however, shortly after CED.

Magnetic iron-oxide nanoparticles (IONPs) have recently been used for CED in rodent models [17,18,24]. The ability to directly image these nanoparticles sensitively with MRI on T2-weighted sequences and their ability to be covalently conjugated to tumor-specific therapeutic agents provide the basis for their use in CED and direct tumor targeting [18]. Due to their size (10 nm core), cell endocytosis and penetration of IONPs through the extracellular matrix in the brain is possible [8,18,25]. We have found that IONPs conjugated to an EGFRvIII antibody can distribute well after CED both intra-tumorally as well as peri-tumorally in human GBM xenografts implanted in rodents and can increase overall animal survival [17]. IONPs remain in the rodent brain for weeks after CED and continue to disperse into the normal brain days after CED potentially targeting the infiltrating GBM cells that reside out the main tumor mass [17].

All of our canine subjects required general anesthesia during the single CED catheter implantation into the brain and during MRI scanning after IONP CED. Each external programmable CED pump was strapped onto the canine subject after being connected to a subcutaneously tunneled catheter (Figure 2). CED studies were performed on our awake canine subjects for up to 24 h and sensitive MRI monitoring of IONP distribution was possible up to 30 d later. While MRI scans were performed on each subject at the completion of each CED procedure, the use of the Medtronic Synchromed II pump could permit MRI scanning during the CED procedure since it is MRI-compatible for real-time CED imaging if needed. These pumps have been used for human intrathecal infusions and a prior human GBM CED trial[1].

Utilizing higher infusion rates (1, 3, or 5 μl/min) did result in leakback along the CED catheter of the IONPs with CED as confirmed by MRI (Figure 3). Our ability to directly image the IONPs by MRI, revealed subarachnoid and intraventricular IONP distribution in

two of our canine subjects (Figure 3). Although only two canines underwent a CED infusion rate of 0.5 μl/min, we found this rate of infusion resulted in the best distribution of the IONPs in both the gray and white matter of the brain with the two canines tested (Figure 4). Dispersion at this rate was also found 5 days after the CED procedure (Figure 5).

All of our canine subjects showed no signs of toxicity or neurologic deficits by clinical examination, as well as hematologic and CSF analysis after IONP CED. Predominant clearance of the bioconjugated cetuximab-IONPs was found at 30 d after CED. The accumulation of iron-filled gitter cells and gemistocytic astrocytes around each catheter site provided evidence for the uptake and clearance of the free and bioconjugated IONPs in the canine brain (Figure 6).

Conclusions

We have demonstrated, for the first time, the CED of magnetic IONPs into the healthy canine brain for distribution/dispersion volume assessment, clearance, and toxicity evaluation. Both free IONPs and cetuximab-conjugated IONPs were used in our canine subjects and could be sensitively monitored by MRI for days after CED. All of our canine subjects showed no signs of central nervous system (CNS) or systemic toxicities after CED treatment. We believe bioconjugated cetuximab-IONPs represent a potential therapeutic agent that could be evaluated in canine patients with spontaneous gliomas after CED. The canine spontaneous glioma model represents one of the best models to study the delivery and efficacy of potential therapeutic agents that could be translated to human GBM patients.

Acknowledgments

Financial support:

This work was supported in part by grants from the NIH (NS053454 to CGH; P50CA128301-01A10003 to HM and CGH, 1U01CA151810-01 to HM, 5R01CA154846-02 to HM), the Georgia Cancer Coalition, Distinguished Cancer Clinicians and Scientists Program (to CGH), and the Dana Foundation (to CGH).

References

1. Kunwar S, Prados MD, Chang SM, et al. Direct intracerebral delivery of cintredekin besudotox (IL13-PE38QQR) in recurrent malignant glioma: a report by the Cintredekin Besudotox Intraparenchymal Study Group. J Clin Oncol. Mar 1; 2007 25(7):837–844. [PubMed: 17327604]
2. Mardor Y, Roth Y, Lidar Z, et al. Monitoring response to convection-enhanced taxol delivery in brain tumor patients using diffusion-weighted magnetic resonance imaging. Cancer Res. Jul 1; 2001 61(13):4971–4973. [PubMed: 11431326]
3. Bobo RH, Laske DW, Akbasak A, Morrison PF, Dedrick RL, Oldfield EH. Convection-enhanced delivery of macromolecules in the brain. Proc Natl Acad Sci U S A. Mar 15; 1994 91(6):2076–2080. [PubMed: 8134351]
4. Allard E, Passirani C, Benoit JP. Convection-enhanced delivery of nanocarriers for the treatment of brain tumors. Biomaterials. Apr; 2009 30(12):2302–2318. [PubMed: 19168213]
5. Lidar Z, Mardor Y, Jonas T, et al. Convection-enhanced delivery of paclitaxel for the treatment of recurrent malignant glioma: a phase I/II clinical study. J Neurosurg. Mar; 2004 100(3):472–479. [PubMed: 15035283]
6. Sampson JH, Archer G, Pedain C, et al. Poor drug distribution as a possible explanation for the results of the PRECISE trial. J Neurosurg. Aug; 2010 113(2):301–309. [PubMed: 20020841]
7. MacKay JA, Deen DF, Szoka FC Jr. Distribution in brain of liposomes after convection enhanced delivery; modulation by particle charge, particle diameter, and presence of steric coating. Brain research. Feb 28; 2005 1035(2):139–153. [PubMed: 15722054]

8. Neeves KB, Sawyer AJ, Foley CP, Saltzman WM, Olbricht WL. Dilation and degradation of the brain extracellular matrix enhances penetration of infused polymer nanoparticles. Brain Res. Nov 14.2007 1180:121–132. [PubMed: 17920047]
9. Vavra M, Ali MJ, Kang EW, et al. Comparative pharmacokinetics of 14C-sucrose in RG-2 rat gliomas after intravenous and convection-enhanced delivery. Neuro Oncol. Apr; 2004 6(2):104–112. [PubMed: 15134624]
10. Chen MY, Hoffer A, Morrison PF, et al. Surface properties, more than size, limiting convective distribution of virus-sized particles and viruses in the central nervous system. J Neurosurg. Aug; 2005 103(2):311–319. [PubMed: 16175862]
11. Sampson JH, Brady ML, Petry NA, et al. Intracerebral infusate distribution by convection-enhanced delivery in humans with malignant gliomas: descriptive effects of target anatomy and catheter positioning. Neurosurgery. Feb; 2007 60(2 Suppl 1):ONS89–98. discussion ONS98–89. [PubMed: 17297371]
12. Varenika V, Dickinson P, Bringas J, et al. Detection of infusate leakage in the brain using real-time imaging of convection-enhanced delivery. J Neurosurg. Nov; 2008 109(5):874–880. [PubMed: 18976077]
13. Saito R, Bringas JR, McKnight TR, et al. Distribution of liposomes into brain and rat brain tumor models by convection-enhanced delivery monitored with magnetic resonance imaging. Cancer Res. Apr 1; 2004 64(7):2572–2579. [PubMed: 15059914]
14. Dickinson PJ, Lecouteur RA, Higgins RJ, et al. Canine spontaneous glioma: A translational model system for convection-enhanced delivery. Neuro Oncol. May 20.2010
15. Sampson JH, Akabani G, Archer GE, et al. Intracerebral infusion of an EGFR-targeted toxin in recurrent malignant brain tumors. Neuro Oncol. Jun; 2008 10(3):320–329. [PubMed: 18403491]
16. Sampson JH, Akabani G, Friedman AH, et al. Comparison of intratumoral bolus injection and convection-enhanced delivery of radiolabeled antitenascin monoclonal antibodies. Neurosurg Focus. 2006; 20(4):E14. [PubMed: 16709019]
17. Hadjipanayis CG, Machaidze R, Kaluzova M, et al. EGFRvIII antibody-conjugated iron oxide nanoparticles for magnetic resonance imaging-guided convection-enhanced delivery and targeted therapy of glioblastoma. Cancer Res. Aug 1; 2010 70(15):6303–6312. [PubMed: 20647323]
18. Wankhede M, Bouras A, Kaluzova M, Hadjipanayis CG. Magnetic nanoparticles: an emerging technology for malignant brain tumor imaging and therapy. Expert Rev Clin Pharmacol. Mar; 2012 5(2):173–186. [PubMed: 22390560]
19. Stoica G, Kim HT, Hall DG, Coates JR. Morphology, immunohistochemistry, and genetic alterations in dog astrocytomas. Vet Pathol. Jan; 2004 41(1):10–19. [PubMed: 14715963]
20. Dickinson PJ, Roberts BN, Higgins RJ, et al. Expression of receptor tyrosine kinases VEGFR-1 (FLT-1), VEGFR-2 (KDR), EGFR-1, PDGFRalpha and c-Met in canine primary brain tumours. Vet Comp Oncol. Sep; 2006 4(3):132–140. [PubMed: 19754810]
21. Higgins RJ, Dickinson PJ, Lecouteur RA, et al. Spontaneous canine gliomas: overexpression of EGFR, PDGFRalpha and IGFBP2 demonstrated by tissue microarray immunophenotyping. J Neurooncol. Dec 5.2009
22. Higgins RJ, Dickinson PJ, LeCouteur RA, et al. Spontaneous canine gliomas: overexpression of EGFR, PDGFRalpha and IGFBP2 demonstrated by tissue microarray immunophenotyping. Journal of neuro-oncology. May; 2010 98(1):49–55. [PubMed: 19967449]
23. Dickinson PJ, LeCouteur RA, Higgins RJ, et al. Canine model of convection-enhanced delivery of liposomes containing CPT-11 monitored with real-time magnetic resonance imaging: laboratory investigation. J Neurosurg. May; 2008 108(5):989–998. [PubMed: 18447717]
24. Perlstein B, Ram Z, Daniels D, et al. Convection-enhanced delivery of maghemite nanoparticles: Increased efficacy and MRI monitoring. Neuro Oncol. Apr; 2008 10(2):153–161. [PubMed: 18316474]
25. Thorne RG, Nicholson C. In vivo diffusion analysis with quantum dots and dextrans predicts the width of brain extracellular space. Proc Natl Acad Sci U S A. Apr 4; 2006 103(14):5567–5572. [PubMed: 16567637]

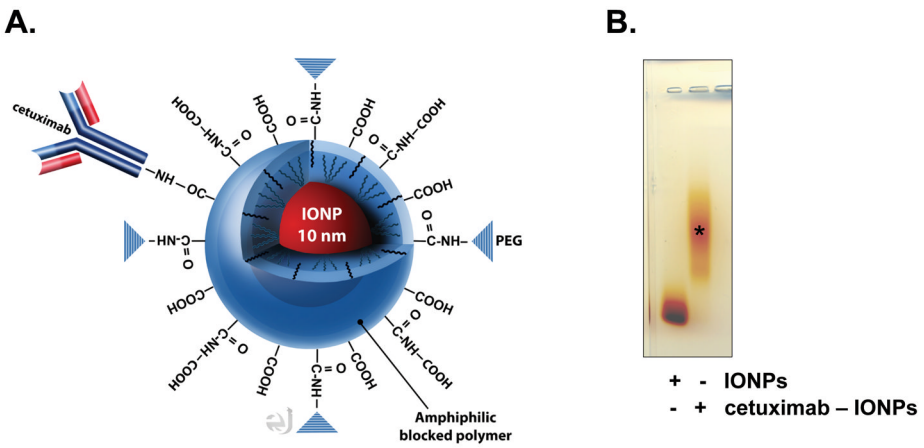

Figure 1. Cetuximab-conjugated IONPs

A., An IONP (shown in red; core size of 10 nm) coated with a biocompatible amphiphilic triblock copolymer [17] bioconjugated to the EGFR monoclonal antibody cetuximab is shown. Bioconjugation of cetuximab is performed to the – COOH of the polymer coating. B., Agarose gel electrophoresis confirming IONP bioconjugation to cetuximab (*). Free IONPs are shown to the left.

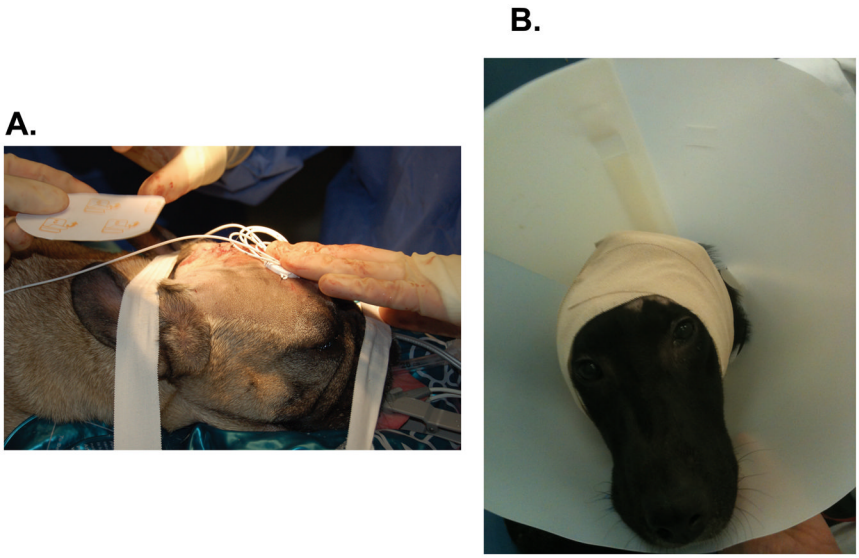

Figure 2. Canine IONP CED setup

A. A single CED catheter is tunneled subcutaneously through the scalp after being placed 1–2 cm into the right frontal lobe through a burr hole. **B.,** Strapping of an external programmable reservoir infusion pump to a canine's head for IONP CED.

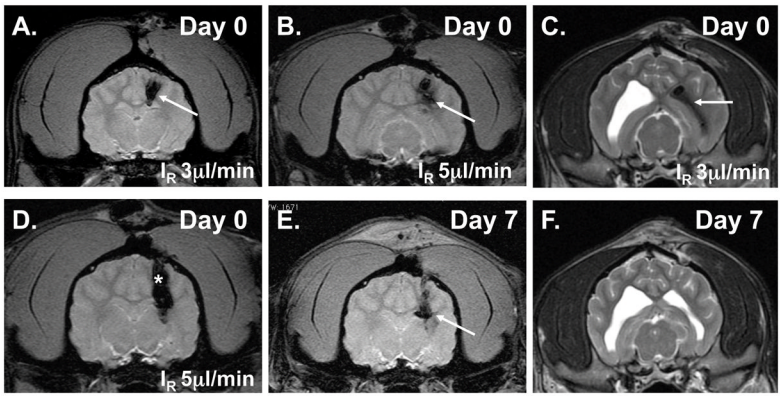

Figure 3. Initial free IONP CED studies in the healthy canine brain (Group 1; 60 min infusions), T2WI (including gradient echo), and IONP MRI contrast effect (shown by arrows)

A., IONP CED (V_i 180μl & I_R 3 μl/min) at day 0. B., IONP CED (V_i 300μl & I_R 5 μl/min) at day 0. C., Intraventricular placement of IONPs after CED. D., Leakback of IONPs along catheter (shown by asterisk) is shown at the higher I_R (5 μl/min). E., Presence of intracerebral IONPs 7 d after CED. F., Clearance of intraventricular IONPs 7 d after CED.

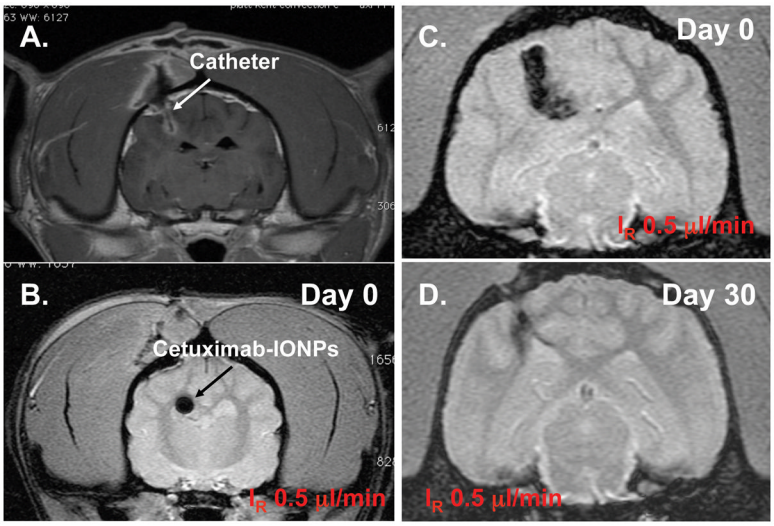

Figure 4. MRI-guided cetuximab-IONP CED in the canine brain (Group 2)

A., T1WI confirming catheter positioning. T2WI showing uniform distribution of IONPs (black arrow) at the lower infusion rate (I_R=0.5 µl/min) for 12 h (B) and greater distribution at 24 h (C). Loss of T2 hypointensity (D) 30 d after CED.

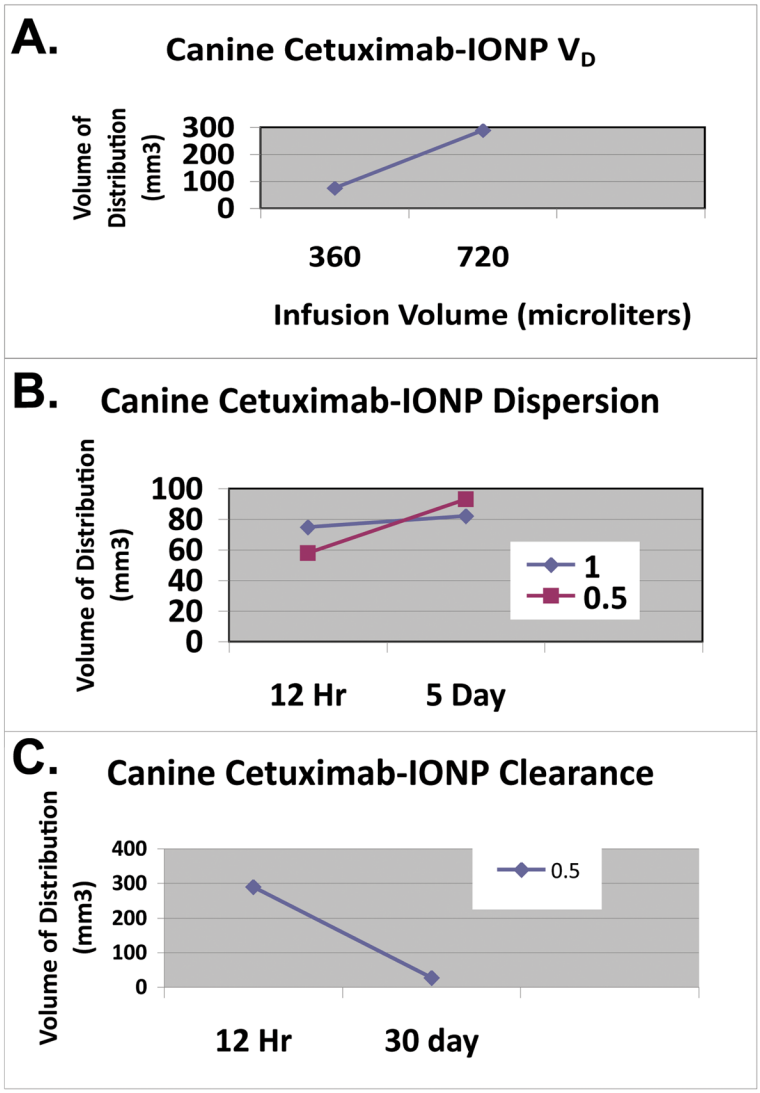

Figure 5. Cetuximab-IONP CED volume of distribution, dispersion, and clearance in the canine brain (Group 2)

A., IONP volume of distribution (V_D) after CED was determined by T_2 contrast (signal drop) present on T2WI. V_D was linearly proportional to the infusion volume (V_I). B., Initial IONP V_D after CED was determined at 12h on day 0 with a CED infusion rate (I_R) of 0.5 or 1.0 μl/min. The V_D was determined 5 d after CED confirming dispersion of the bioconjugated IONPs at both I_R. Greater IONP dispersion was found at the 0.5 μl/min rate. C., Clearance of IONPs was determined by T2WI V_D comparison at 12 h and 30 d after CED of IONPs (0.5 μl/min for 24 h). T_2 contrast is almost completely gone at 30 d.

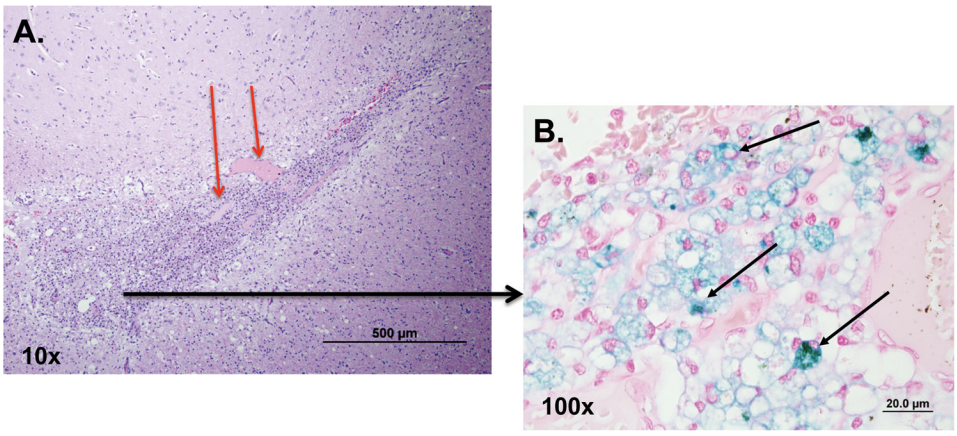

Figure 6. Histopathologic analysis of the catheter tract in the canine brain 30 d after IONP CED

A., Hematoxylin and eosin stained brain section of the CED catheter site surrounded by gitter cells (phagocytizing microglia) (10 x). Neovascularization is seen as well (shown by red arrows). B., Magnified view (100 x) revealing the presence of iron-filled gitter cells (black arrows) after Perl's blue staining of brain section.